Smart Structures and Systems, *Vol. 24, No. 4 (2019) 507-524*
DOI: https://doi.org/10.12989/sss.2019.24.4.507

Bayesian forecasting approach for structure response prediction and load effect separation of a revolving auditorium

Zhi Ma, Chung-Bang Yun, Yan-Bin Shen, Feng Yu,
Hua-Ping Wan and Yao-Zhi Luo*

College of Civil Engineering and Architecture, Zhejiang University, Hangzhou, Zhejiang, China

(Received January 28, 2019, Revised May 27, 2019, Accepted May 31, 2019)

Abstract. A Bayesian dynamic linear model (BDLM) is presented for a data-driven analysis for response prediction and load effect separation of a revolving auditorium structure, where the main loads are self-weight and dead loads, temperature load, and audience load. Analyses are carried out based on the long-term monitoring data for static strains on several key members of the structure. Three improvements are introduced to the ordinary regression BDLM, which are a classificatory regression term to address the temporary audience load effect, improved inference for the variance of observation noise to be updated continuously, and component discount factors for effective load effect separation. The effects of those improvements are evaluated regarding the root mean square errors, standard deviations, and 95% confidence intervals of the predictions. Bayes factors are used for evaluating the probability distributions of the predictions, which are essential to structural condition assessments, such as outlier identification and reliability analysis. The performance of the present BDLM has been successfully verified based on the simulated data and the real data obtained from the structural health monitoring system installed on the revolving structure.

Keywords: Bayesian dynamic linear model; data-driven method; response prediction; load effect separation; revolving structure; structural health monitoring

1. Introduction

In this study, a Bayesian dynamic linear model based on the structural health monitoring data is presented for the stress response prediction and load effect separation of a revolving auditorium structure. This structure is a steel truss structure for outdoor musical performances in the area of Mt. Wuyi in China. It can revolve on a track system to provide 360-degree panoramic views of the stage show and background natural landscapes. An extensive structural health monitoring (SHM) system, primarily consisting of 55 wireless channels of wireless strain sensors, was installed after the completion of construction in 2015 to assure the safety of the audience, which can reach a maximum capacity of 2000 people, as well as the integrity of the structure (Luo *et al.* 2014). This structure is subjected to various loads, such as structural weights, equipment load, audience load, temperature load, operational load, movements of a large number of performers, and to harsh outdoor environmental conditions.

In recent decades, there have been numerous studies on various types of SHM systems with various kinds of sensors and their applications to civil engineering structures (Siringoringo and Fujino 2009, Rice *et al.* 2010, Pakzad 2010, Zonta *et al.* 2010, Min *et al.* 2010, Shen *et al.* 2013, Wang *et al.* 2018, Wu *et al.* 2018). Vibration data such as accelerations have been commonly used for the assessment of global behavior and damage detections (Hua *et al.* 2009, Cho *et al.* 2010, Shinozuka *et al.* 2010, Ni *et al.* 2011, Kim and Lynch 2012, Kim *et al.* 2016). However, static data such as strains, have been widely used in local monitoring for the damage detection and the condition assessment on structural members and joints (Chen *et al.* 2004, Strauss *et al.* 2008, Catbas *et al.* 2008, Zhu and Frangopol 2013, Zhang *et al.* 2017, Wan and Ni 2018a).

The condition assessments of structures have traditionally been carried out by the model-based approach, such as finite element (FE) model updating (Brownjohn *et al.* 2003, Skolnik *et al.* 2006, Beck 2010, Chung *et al.* 2012). However, the revolving structure is subjected to various uncertainties in the loading, particularly the audience load and the wheel-rail contact conditions during and after the rotating operations. Hence it is difficult to create a reliable FE model for the structure while in service. A data-driven condition assessment approach is taken in this study. There are many studies that have examined this approach, for instance time series methods such as the autoregressive model (Noh and Nair 2009, Gul and Catbas 2009), the autoregressive moving average model (Zheng and Mita 2008, Carden and Brownjohn 2008), the machine learning algorithms (Yun and Bahng 2000, Lee *et al*. 2005, Min *et al.* 2012, Lin *et al.* 2017, Kim *et al.* 2018), the Gaussian process-based Bayesian model (Wan and Ni 2018a, b), and the Beyesian inference (Jin 2019). The main procedure of those methods is to build a proper prediction model for the structural response, and then compare the predictions with the current measurements. The occurrence of outliers indicates abnormal changes in the structure.

*Corresponding author, Professor
E-mail: luoyz@zju.edu.cn

ISSN: 1738-1584 (Print), 1738-1991 (Online)

Accurate predictions of structural responses for different kinds of loads are highly essential for reliable condition assessment of the structures in-serve. However, structures are always under varying environmental and operational conditions. It has been often reported that the structural response changes caused by environmental loads (e.g., temperature) can conceal the damage-induced changes (Sohn 2006, Xu *et al*. 2010, Xia *et al*. 2012). If those load effects are not fully understood, false structural condition assessment may occur. Many studies have been focused on separation of the load effects and extraction of the environmental effects to have a reliable assessment of the structural condition (Jin *et al.* 2015, Kromanis and Kripakaran 2016, Zhu *et al.* 2018, Zhu *et al*. 2019).

The main objective of this study is to develop a data-driven method for the prediction of stress response and the separation of various load effects for the revolving auditorium structure. A Bayesian dynamic linear model (BDLM) (West and Harrison 1997) is employed in which the predictions for the responses and the state variables representing various load effects can be updated based on the new monitoring data at each time step. The BDLM is capable of modeling structural behavior under operational conditions by including various components, such as trend, seasonal, and regression components. There have seen a large volume of research works on the BDLM for various applications in the SHM field, such as prediction of structural performance (Wang and Liu 2010), modeling of real-time structural response and external effects (Goulet 2017, Goulet and Koo 2018, Wang *et al*. 2019), and detection of unexpected changes (Zhang *et al*. 2018). However, the BDLM variants used in the above studies are not suitable for the structures subjected to a large-scale temporary load (such as the audience load in this study). Furthermore, those models treat the variance of the observation noise as a constant value, which is not reasonable to the present structure subjected to various uncertainties related to environmental and operational conditions. Hence, a novel BDLM needs to develop to better characterize the temporary audience load effect and the uncertainty related to the daily revolving operation of a revolving auditorium.

Three improvements are introduced to the BDLM for the revolving auditorium in this study. First, a classificatory regression BDLM is employed to address the unknown temporary audience load effect. Then, the variance of observation noise is treated as a random variable and updated along with other random variables using the Bayesian inference at each time step. Finally, component discount factors are introduced to the covariance matrix of the system noise to address the different uncertainties in each state parameter, so that the load separation result can be improved. Effects of those improvements are evaluated regarding the root mean square errors, standard deviations, and 95% confidence intervals of the predictions. Bayes factors are used for evaluation of the probability distributions of the predictions. Verification of the present BDLM is successfully carried out using the simulation data and the real monitoring data obtained from the long-term online SHM system on the structure.

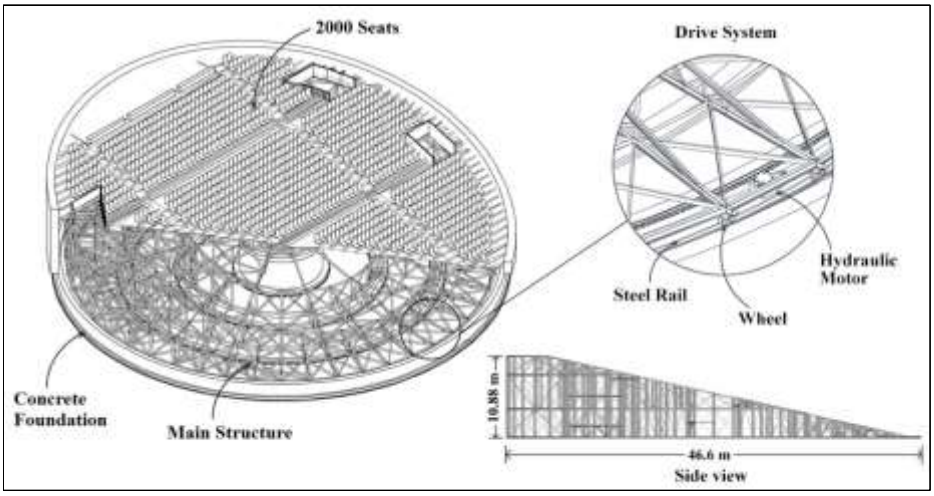

(a) Revolving structure and its drive system

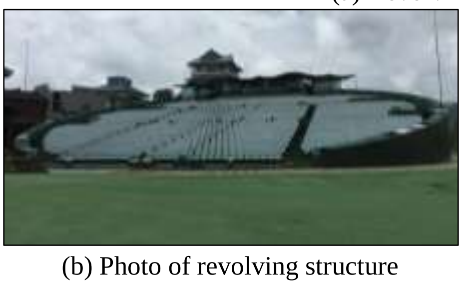

(b) Photo of revolving structure

(c) Photo of wheel-rail system

Fig. 1 Revolving structure and its wheel-rail system

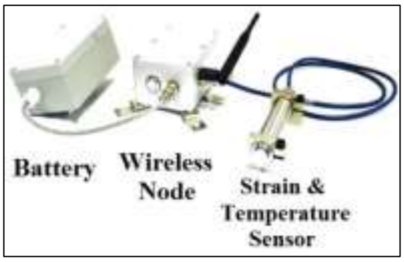

(a) Wireless sensor node

(b) Sensor installation

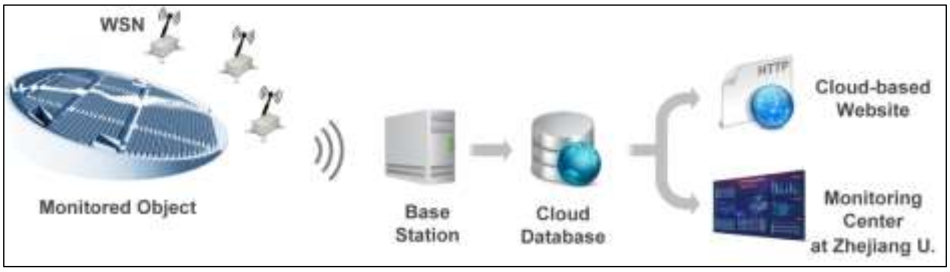

(c) Wireless monitoring system

Fig. 2 The wireless monitoring system of revolving auditorium

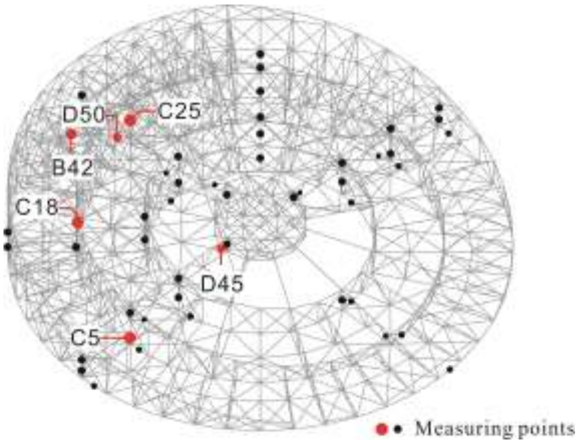

Fig. 3 Layout of strain sensors on the revolving structure

2. Revolving auditorium and its monitoring system

2.1 Revolving auditorium

In this study, the response prediction and load effect separation are carried out on a large revolving structure using a Bayesian dynamic linear model. The structure is an auditorium for outdoor musical performances, *Impression Dahongpao*, in the area of Mt. Wuyi in China. As shown in Fig. 1, the auditorium revolves on 4 circular steel rails. It is driven by a hydraulic motor drive system and has a maximum rotation speed of 1.2 $°/s$. During the show, it carries as many as 2000 audience members and provides 360-degree views of the stage show and the background natural landscape. The main structure of the auditorium is a steel truss structure, which has a maximum height of 10.88 m, a diameter of 46.6 m, and a weight of 520 tons. More details about this structure can be found in the reference (Luo *et al.* 2014).

2.2 Wireless monitoring system

A long-term wireless SHM system has been installed on this structure for online monitoring by Zhejiang University (Luo *et al.* 2014). Similar SHM systems have been used for several other large-scale structures (Shen *et al.* 2013, Zhang *et al.* 2017). The wireless system is suitable for this revolving auditorium because it does not need to consider wiring problems in the rotating of the structure. Fig. 2 shows the wireless sensor node, sensor installation, and the wireless monitoring system. The measured strain and temperature data are transmitted to the base station through wireless nodes. After finishing measurements at each time point, all of the monitored data are uploaded to the monitoring cloud database, and then displayed at the cloud-based websites and the monitoring center at Zhejiang University.

There are a total of 55 vibrating wire strain sensors installed on the main structure, as shown in Fig. 3. Among

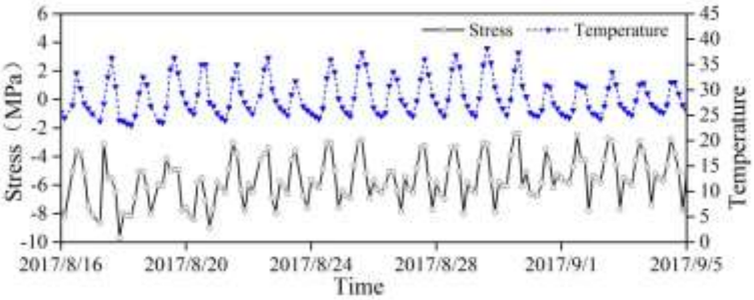

Fig. 4 Examples of measured stress and temperature data at C25

them, 34 are installed on column members, 12 are on beam members, and 9 are on diagonal members. Strain and temperature are measured 8 times at every 3 hours each day, and the strain data are converted into stresses. The measurement at 21:00 is during the musical performance; therefore, the last monitoring data on each day include the audience load effect. The monitoring data at 6 big red points marked in Fig. 3 are analyzed for the response prediction and load effect separation in this study. C4, C18 and C25 are column members, B42 is a beam member, and D45 and D50 are diagonal members. Fig. 4 shows the stress and temperature data at C25 during a period of 16 August – 5 September 2017. The stress responses are mainly influenced by the temperature change and the audience loads at the end of the days.

3. Methodology

3.1 Bayesian forecasting and dynamic linear model

3.1.1 Dynamic linear model

The dynamic linear model (DLM) is commonly used for time series analysis in Bayesian forecasting. If y_t denotes the observation variable at time t and $\boldsymbol{\theta}_t$ denotes the $n \times 1$ state vector, the general DLM is defined as (West and Harrison 1997)

Observation equation

$$y_t = \boldsymbol{F}_t'\boldsymbol{\theta}_t + \nu_t, \qquad \nu_t \sim N[O, V_t] \tag{1}$$

System equation

$$\boldsymbol{\theta}_t = \boldsymbol{G}_t\boldsymbol{\theta}_{t-1} + \boldsymbol{\omega}_t, \qquad \boldsymbol{\omega}_t \sim N[\boldsymbol{O}, \boldsymbol{W}_t] \tag{2}$$

Initial information

$$(\boldsymbol{\theta}_0 \mid D_0) \sim N[\boldsymbol{m}_0, \boldsymbol{C}_0] \tag{3}$$

where y_t and $\boldsymbol{\theta}_t$ are a random variable and a vector; ν_t is the observation noise that represents the measurement error; $\boldsymbol{\omega}_t$ is the system noise or modeling error that is treated as a stochastic change in the state vector $\boldsymbol{\theta}_t$; ν_t and $\boldsymbol{\omega}_t$ are generally assumed as normal (Gaussian) random variables with zero means and variance V_t and covariance matrix $\boldsymbol{W}_t$; $\boldsymbol{F}_t$ ($n \times 1$) is the known observation vector; and $\boldsymbol{G}_t$ ($n \times n$) is the known state transition matrix. The initial distribution for $\boldsymbol{\theta}_t$ at time 0 may be determined based on the information from the past, as $\boldsymbol{m}_0$ and $\boldsymbol{C}_0$ are the mean value and covariance matrix, respectively. With Eqs. (1) and (2), the updating relationship between the measurement and unknown state parameters can be obtained.

There are many different forms for the DLM, such as a trend model, regression model, season model, and their combinations (Goulet 2017). The regression DLM is used as the basic DLM for the revolving auditorium in this study, which is defined as follows

Observation equation

$$y_t = \alpha_t + \gamma_t x_t + \nu_t, \qquad \nu_t \sim N[0, V_t] \tag{4}$$

System equation

$$\boldsymbol{\theta}_t = \begin{Bmatrix} \alpha \\ \gamma \end{Bmatrix}_t = \begin{Bmatrix} \alpha \\ \gamma \end{Bmatrix}_{t-1} + \boldsymbol{\omega}_t, \qquad \boldsymbol{\omega}_t \sim N[\boldsymbol{O}, \boldsymbol{W}_t] \tag{5}$$

where y_t is the observed structure response at time t; α_t denotes the basic structural response due to the self-weight and dead loads; x_t is a measurable regression variable related to a time-varying load such as temperature; and γ_t is a regression parameter for x_t. Therefore $\gamma_t x_t$ represents the structure response caused by x_t. In Eqs. (4) and (5), F_t and G_t are taken as $F_t' = \langle 1, x_t \rangle$ and $\mathrm{G}_t = I_{(2\times 2)}$. The state parameters α_t and γ_t will be updated and the posterior probability distribution will be estimated based on the newly monitored data y_t at each time step.

3.1.2 Bayesian forecasting

The posterior probability distributions for the state parameters at t and the distribution for the predicted structural response at the next time step t+1 can be obtained by Bayesian inference. The inference procedures of the general Bayesian dynamic linear model (BDLM) can be summarized as (West and Harrison 1997)

(a) With posterior distribution for $\boldsymbol{\theta}_{t-1}$: $(\boldsymbol{\theta}_{t-1} \mid D_{t-1}) \sim N[\boldsymbol{m}_{t-1}, \boldsymbol{C}_{t-1}]$, where D_{t-1} denotes the past observations up to y_{t-1}; and $\boldsymbol{m}_{t-1}$ and $\boldsymbol{C}_{t-1}$ are based on the previous inference results at t-1.

(b) The prior distribution for $\boldsymbol{\theta}_t$ at t can be obtained as $(\boldsymbol{\theta}_t \mid D_{t-1}) \sim N[\boldsymbol{a}_t, \boldsymbol{R}_t]$, where $\boldsymbol{a}_t = \boldsymbol{G}_t\boldsymbol{m}_{t-1}$ and $\boldsymbol{R}_t = \boldsymbol{G}_t\boldsymbol{C}_{t-1}\boldsymbol{G}_t' + \boldsymbol{W}_t$.

(c) A one-step forecast distribution for y_t can be estimated as $(y_t \mid D_{t-1}) \sim N[f_t, Q_t]$, where $f_t = \boldsymbol{F}_t' \boldsymbol{a}_t$ and $Q_t = \boldsymbol{F}_t' \boldsymbol{R}_t \boldsymbol{F}_t + V_t$.

(d) With new observation y_t at t, the posterior distribution for $\boldsymbol{\theta}_t$ can be obtained as $(\boldsymbol{\theta}_t \mid D_t) \sim N[\boldsymbol{m}_t, \boldsymbol{C}_t]$, where $\boldsymbol{m}_t = \boldsymbol{a}_t + \boldsymbol{A}_t e_t$; $\boldsymbol{C}_t = \boldsymbol{R}_t - \boldsymbol{A}_t Q_t \boldsymbol{A}_t'$; $\boldsymbol{A}_t = \boldsymbol{R}_t \boldsymbol{F}_t Q_t^{-1}$; and the one-step forecast error $e_t = y_t - f_t$.

3.1.3 Load effect separation

After obtaining the posterior distribution of each state parameter, the posterior distribution of the component response can be obtained by model decomposition. If y_{ti} denotes the structure response caused by the i^{th} load, then its posterior distributions are as follows

$$y_{ti} \sim N[\hat{\boldsymbol{F}}_{ti}' \boldsymbol{m}_t, \quad \hat{\boldsymbol{F}}_{ti}' \boldsymbol{C}_t \hat{\boldsymbol{F}}_{ti}] \tag{6}$$

$$\hat{\boldsymbol{F}}_{ti}' = \langle 0, \cdots 0, F_{ti}, 0, \cdots, 0 \rangle \tag{7}$$

where $\boldsymbol{m}_t$ and $\boldsymbol{C}_t$ are the posterior mean and covariance of the state vector; $\hat{\boldsymbol{F}}_{ti}$ is a column vector, whose i^{th} element F_{ti} is equal to the i^{th} element of the observation vector $\boldsymbol{F}_t$, and the remaining elements are 0. With the formulation above, the different load effects can be separated from the monitored structure response. For example, the environmental load influence can be separated from the response of the structure. Then by eliminating the environmental load influence, the structure change or damage can be identified more clearly. At the same time, the effect of the environmental load can be analyzed accurately.

3.2 BDLM for the revolving auditorium

3.2.1 Classificatory regression BDLM

If the wheel-rail influence is considered to be the uncertainty, the revolving auditorium is mainly subjected to basic, temperature, and temporary audience loads. However, the audience load during the performance is very difficult to measure; hence, the regression BDLM defined by Eqs. (4) and (5) is modified as a classificatory regression model in this study. By introducing a classificatory regression variable z_t as

$$z_t = \begin{cases} 1, & \text{under the temporary load} \\ 0, & \text{no temporary load} \end{cases} \tag{8}$$

a classificatory regression BDLM is defined as

Observation equation

$$y_t = \langle 1, x_t, z_t \rangle \begin{Bmatrix} \alpha \\ \gamma \\ \lambda \end{Bmatrix}_t + \nu_t = \alpha_t + \gamma_t x_t + \lambda_t z_t + \nu_t \tag{9}$$

System equation

$$\boldsymbol{\theta}_t = \begin{Bmatrix} \alpha \\ \gamma \\ \lambda \end{Bmatrix}_t = \begin{Bmatrix} \alpha \\ \gamma \\ \lambda \end{Bmatrix}_{t-1} + \boldsymbol{\omega}_t \tag{10}$$

where λ_t is the temporary load effect, $\boldsymbol{\theta}_t' = \langle \alpha_t, \gamma_t, \lambda_t \rangle$, and $\boldsymbol{F}_t' = \langle 1, x_t, z_t \rangle$. With the classificatory regression BDLM, the temporary load parameter λ_t will be updated along with the others (α_t and γ_t) based on the observation y_t. However, when there is no temporary load, the prediction model becomes an ordinary regression BDLM and the parameter λ_t is no longer updated. This classificatory regression BDLM can also be used for other temporary loads, such as snow load.

3.2.2 Improvement for V_t estimation

The variance of the observation noise V_t, which is to be predescribed, will directly influence the predicted variance of y_t. However, it is very difficult to estimate it in real structure monitoring. Therefore, in this study, V_t is considered as a random variable and estimated during the forecast inference. According to Bayes' theory, the variance of a normal random variable follows an inverse-gamma distribution, whereas its mean value follows Student's *t*-distribution (Lindley 1972). The forecast inference procedure by treating V_t as a random variable can be summarized as follows (West and Harrison 1997):

(a) Posterior distribution at time t-1

$$(V_{t-1} \mid D_{t-1}) \sim IG[n_{t-1}/2, d_{t-1}/2] \tag{11}$$

$$S_{t-1} = E(V_{t-1}) = (d_{t-1}/2)/(n_{t-1}/2 - 1) \tag{12}$$

$$(\boldsymbol{\theta}_{t-1} \mid D_{t-1}) \sim T_{n_{t-1}}[\boldsymbol{m}_{t-1}, \boldsymbol{C}_{t-1}] \tag{13}$$

where $V_{t\text{-}1}$ is the variance of the observation noise ν_{t-1}, which follows the inverse gamma distribution with the shape and scale parameters $n_{t-1}/2$ and $d_{t-1}/2$; S_{t-1} is the expected value of $V_{t\text{-}1}$; and n_{t-1} is the number of degrees of freedom of Student's *t* variable $\boldsymbol{\theta}_{t-1}$.

(b) Prior distribution at time t

$$(\boldsymbol{\theta}_t \mid D_{t-1}) \sim T_{n_{t-1}}[\boldsymbol{a}_t, \boldsymbol{R}_t] \tag{14}$$

where $a_t + G_t m_{t-1}$ and $R_t = G_t C_{t-1} G_t' + W_t$.

(c) One-step forecast distribution of y_t

$$(y_t \mid D_{t-1}) \sim T_{n_{t-1}}[f_t, Q_t] \tag{15}$$

where $f_t = F_t' a_t$ and $Q_t = F_t' R_t F_t + S_{t-1}$.

(d) Posterior distribution at time t

$$(V_t \mid D_t) \sim IG[n_t/2, d_t/2] \tag{16}$$

$$S_t = E(V_t) = (d_t/2)/(n_t/2 - 1) \tag{17}$$

$$(\boldsymbol{\theta}_t \mid D_t) \sim T_{n_t}[\boldsymbol{m}_t, \boldsymbol{C}_t] \tag{18}$$

where $d_t = d_{t-1} + S_{t-1}e_t^2 / Q_t$; $n_t = n_{t-1} + 1$; $e_t = y_t - f_t$; $\boldsymbol{m}_t = \boldsymbol{a}_t + \boldsymbol{A}_t e_t$; $\boldsymbol{A}_t = \boldsymbol{R}_t \boldsymbol{F}_t Q_t^{-1}$; and $\boldsymbol{C}_t = (S_t / S_{t-1})(\boldsymbol{R}_t - \boldsymbol{A}_t Q_t \boldsymbol{A}_t')$.

In this inference procedure, S_t is the posterior estimation for the observation error variance V_t, which is continually updated along with other parameters. It can be seen from Eqs. (15) and (18) that S_t directly affects the results of Q_t and $\boldsymbol{C}_t$, which are covariances of the predicted values for y_t and $\boldsymbol{\theta}_t$.

3.2.3 Component discount factors for $\boldsymbol{W}_t$

The covariance matrix of the system noise $\boldsymbol{W}_t$, which is also to be predescribed, will determine the level of stochastic change in the state vector $\boldsymbol{\theta}_t$. The discount factor δ (West and Harrison 1997) has been customarily applied to the system covariance $\boldsymbol{W}_t$ as

$$\boldsymbol{W}_t = \boldsymbol{G}_t \boldsymbol{C}_{t-1} \boldsymbol{G}_t' (1-\delta) / \delta \tag{19}$$

Then, $\boldsymbol{R}_t$ in Eq. (14) becomes

$$\boldsymbol{R}_t = \boldsymbol{G}_t \boldsymbol{C}_{t-1} \boldsymbol{G}_t' + \boldsymbol{W}_t = \boldsymbol{G}_t \boldsymbol{C}_{t-1} \boldsymbol{G}_t' / \delta \tag{20}$$

Discount factor $\delta \in (0,1]$ denotes the ratio of the covariance of the state vector $\boldsymbol{\theta}_t$ before and after considering the system noise $\boldsymbol{\omega}_t$. If $\delta = 1$, $\boldsymbol{W}_t = 0$ and the state parameters do not change, which means the BDLM is static. The smaller δ is, the larger $\boldsymbol{W}_t$ is, which means that the state vector is subjected to a greater change. Usually, δ is determined by a parametric analysis. In real structures, the state parameters may have the different variations. For example, a state parameter α_t for the basic static load may be almost constant, while other parameter λ_t related to temporary audience load varies significantly. Therefore, co mponent discount factors are introduced for $\boldsymbol{W}_t$ in this study as

$$\boldsymbol{W}_t = \begin{bmatrix} P_{11,t}(1-\delta_1)/\delta_1 & 0 & 0 \\ 0 & P_{22,t}(1-\delta_2)/\delta_2 & 0 \\ 0 & 0 & P_{33,t}(1-\delta_3)/\delta_3 \end{bmatrix} \tag{21}$$

where $P_{ii,t}$ is the i^{th} diagonal element of $\boldsymbol{P}_t = \boldsymbol{G}_t \boldsymbol{C}_{t-1} \boldsymbol{G}_t'$; δ_i is the component discount factor for the i^{th} state parameter defined in Eq. (10).

3.3 Performance indices

The performance of the BDLMs is evaluated using two indices i.e., the root mean square error and the Bayes factor. The root mean square error (RMSE) of the prediction is defined as

$$RMSE = \sqrt{\frac{\sum_{t=1}^{n_t}(y_t - f_t)^2}{n_t}} \tag{22}$$

where y_t is the measured structural response, and f_t is the predicted value as in Eq. (15). The RMSE denotes the accuracy of the predicted mean value.

The Bayes factor (Jeffreys 1961) is used to compare the predicted probability density functions (PDF) for two models M_1 and M_0. If $p_1(y_t|D_{t-1})$ and $p_0(y_t|D_{t-1})$ are the PDF values of M_1 and M_0 at y_t, the Bayes factor for M_1 versus M_0 is defined as

$$H_t = \frac{p_1(y_t \mid D_{t-1})}{p_0(y_t \mid D_{t-1})} \tag{23}$$

If $H_t > 1$, M_1 gives a higher probability density for y_t than M_0, which means M_1 is better for y_t than M_0.

For the overall model assessment for t_n time steps, the cumulative Bayes factor is defined assuming independent observational noise as

$$CH(t_n) = \prod_{r=1}^{t_n} H_r = \frac{p_1(y_t, y_{t-1}, \cdots, y_1 \mid D_0)}{p_0(y_t, y_{t-1}, \cdots, y_1 \mid D_0)} \tag{24}$$

where $CH(t_n)$ denotes the overall prediction performance of M_1 at t_n relative to M_0. Eq. (24) can be changed into the log-cumulative Bayes factor at time t as

$$LCH(\mathrm{t}) = \log[CH(t)] = \sum_{r=1}^{t} \log(H_r) \tag{25}$$

If $LCH(t)$ is increasing with time, which means $\log(H_r) > 0$, M_1 can be judged to be better than M_0.

4. Simulation analysis for verification

4.1 FE model and response simulation

For stress response simulation, an FE model was constructed using the ANSYS package based on the design information of the auditorium structure as shown in Fig. 3. Beam and truss elements are used for modeling the steel members with density of 7.9×10^3 kN/m^3 and elastic modulus of 2.06×10^{11} Pa. The spring elements are used for modeling wheel-rail boundary conditions. Considering the outer rubber layer of a steel wheel, its stiffness is approximately taken as 1×10^9 N/m (equivalent to a similar rubber support) in the vertical direction. On the other hand, it is taken as 1×10^5 N/m in the circular and radial directions, so that the rotation (revolving) frequency of auditorium structure can be equivalent to the measured value. There are a total of 1171 nodes and 2964 elements. Three different load sequences containing 160 data points for 20 days are applied to the FE model and the stress responses are obtained 8 times a day, similar to the monitoring schedule for the real structure. Load 1 is the basic load consisting of the self-weight of the structure and uniform static load on the auditorium floor. The uniform static load is assumed to have a normal distribution of $N(1.5, 0.015)$ in kN/m^2. The mean value of 1.5 kN/m^2 is the load used in the design for the self-weight of the floor, seats and other equipment. The standard deviation of 0.015 kN/m^2 is used to consider the

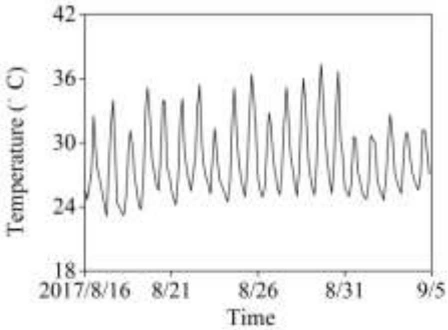

(a) Temperature variation

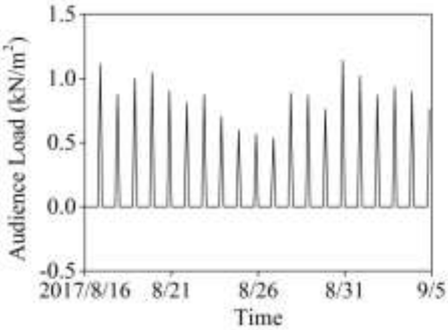

(b) Audience load at 21:00

Fig. 5 Temperature and audience load variations in simulation

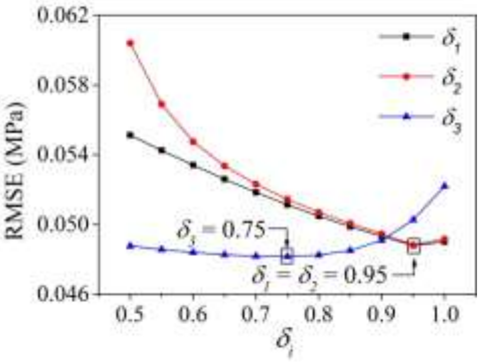

(a) RMSE for component δ_i of CRICM

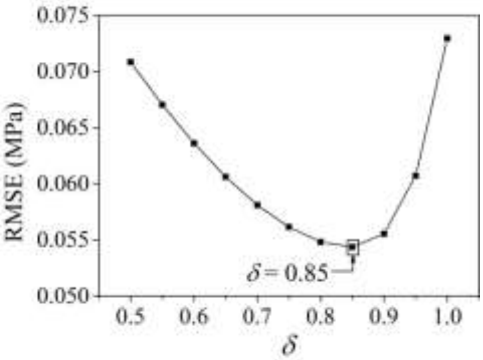

(b) RMSE for overall δ of CRIM

Fig. 6 RMSE of the prediction for different discount factors on Member C25

uncertainty induced by the wheel-rail contact condition. Load 2 is the temperature load shown in Fig. 5(a), which was defined based on the real temperature measurement shown in Fig. 4. Load 3 is the uniform audience load on the floor, as shown in Fig. 5(b), which is applied only at the time instance of 21:00 on each day. It was obtained based on a rough estimation of the number of audiences on each day. The stress responses were simulated on 6 members marked in Fig. 3, and used to build the BDLM. Measurement noises are added to the simulation data, which are assumed to be white noises with zero means and standard deviations with 20% level of the RMS values of the simulated responses. The noise level was approximately estimated based on the real measurement data, whereas the effects of different noise levels are also discussed in Section 4.3.3.

4.2 Establishment of BDLMs for comparative study

To investigate the effectiveness of the model improvements, 4 different BDLMs are considered, as shown in Table 1 CRICM represents the classificatory regression BDLM with improvements for V_t estimation and component discount factors for $\boldsymbol{W}_t$. CRIM denotes the classificatory regression BDLM with improvement for V_t estimation and an overall discount factor for whole $\boldsymbol{W}_t$. On the other hand, CRM represents the classificatory regression BDLM with a constant V_t and an overall discount factor, and RM stands for the basic regression BDLM with a constant V_t and an overall discount factor.

First, the best discount factors were determined for 4 BDLMs using the RMSE for the first 50 stress data. As shown in Fig. 6(a) for C25, the best component discount factors are found to be $\delta_1 = \delta_2 = 0.95$, and $\delta_3 = 0.75$, which indicates that the audience effect has more variation than the basic and temperature effects. For other members, the best δ_1 and δ_2 are also found to be almost same as 0.95. However those for δ_3 are 0.7, 0.8, 0.9, 0.8, and 0.6 for C5, C18, B42, D45, and D50, respectively. These results show that the sensitivity of the audience load varies significantly with different members. Fig. 6(b) shows that the best overall discount factor for C25 in CRIM is $\delta = 0.85$, whereas those for C5, C18, B42, D45, and D50 are obtained as 0.8, 0.9, 0.9, 0.9, and 0.8, respectively. The best overall discount factors for 6 members in CRM are the same as those in CRIM. On the other hand, the overall discount factors vary for different members in RM as 0.95, 0.95, 0.9, 0.9, 0.95, and 0.85 for C5, C18, C25, B42, D45, and D50, respectively.

Table 1 Four different BDLMs

Models	Classificatory regression component	Improvement for V_t estimation	Component discount factors for $\boldsymbol{W}_t$
CRICM	√	√	√
CRIM	√	√	x
CRM	√	x	x
RM	x	x	x

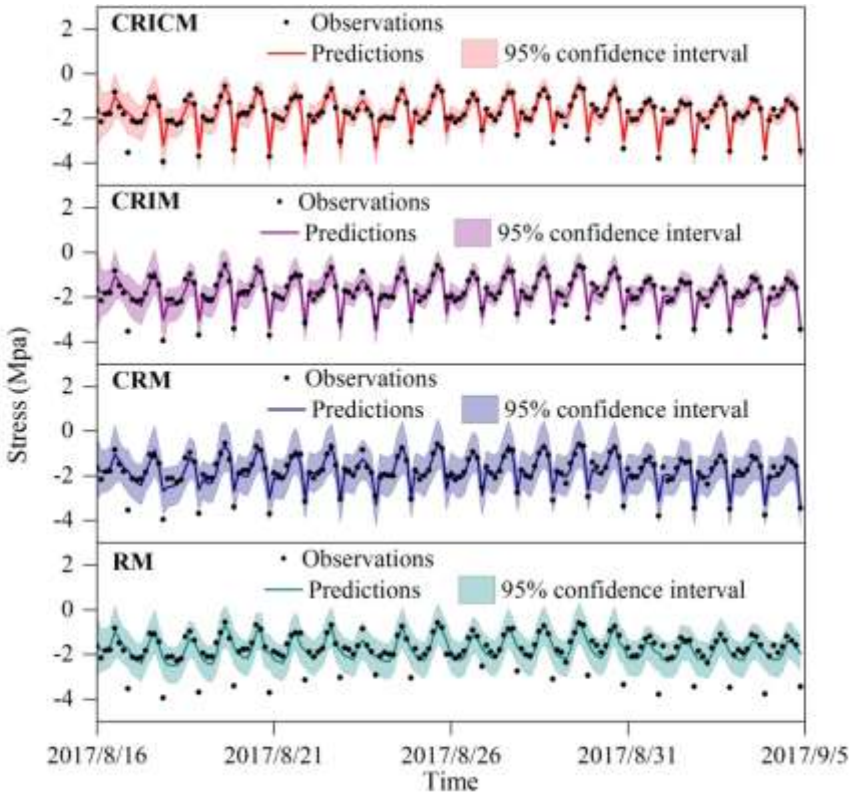

Fig. 7 Stress response predictions for C25 by four BDLMs based on simulation data

4.3 Prediction of stress response

4.3.1 Mean response and RMSE

Fig. 7 shows example cases of the predicted stress responses for a column member C25 by different BDLMs. The initial values for the basic load effect α_0 and temperature coefficient γ_0 are obtained as -2.5 MPa and 0.15 MPa/^{o}C by a regression analysis of the first 7 data points. The initial value for the audience load effect is taken as $\lambda_0 = 0$. For CRICM and CRIM, the initial distribution for the observation noise variance is taken as $V_0 \sim \mathrm{IG}(2, 0.1\mathrm{MPa}^2)$, with $E(V_0) = 0.1\mathrm{MPa}^2$. On the other hand, the variance for CRM and RM is taken as a constant, with $V_t = 0.1\,\mathrm{MPa}^2$. The predicted stresses by CRICM, CRIM and CRM are found to be very close to the observation, whereas the results of CRICM and CRIM converge more quickly than those of CRM. The predicted stress by RM has the largest difference from the observation, especially when the structure is subjected to audience loads. When there is no audience load, the predictions by RM and CRM are basically the same.

Table 2 shows the RMSEs of the predicted stresses for the last 15 days on 6 members by different BDLMs. The RMSE levels of the predictions are found to be very small in the range of 5-8% and 2-6% in comparison with the means and the ranges ($|y_{max}$-$y_{min}|$) of the observations, respectively, except for RM. It is more relevant to compare the RMSE level with the range of the observations, because the RMSE is regarding to the observation which varies significantly with time. The RMSEs of CRICM are the smallest. However, for a beam member B42, the RMSEs by all models are almost the same, because for the beam member, the stress response caused by the audience load is very small. In summary, the CRICM gives the smallest predicted errors compared with the other BDLMs, although its RMSE levels are fairly close to those of CRIM and CRM.

Table 2 RMSEs and standard deviations of the predicted stresses (unit: MPa)

Members	Measured Data		RMSEs of Predictions			
	Mean	$\|y_{max}-y_{min}\|$	CRICM	CRIM	CRM	RM
C5	-3.64	3.38	0.17* (0.20**)	0.19 (0.22)	0.19 (0.36)	0.84 (0.29)
C18	-2.32	3.76	0.18 (0.20)	0.19 (0.21)	0.19 (0.36)	0.74 (0.31)
C25	-1.78	3.40	0.18 (0.18)	0.20 (0.21)	0.20 (0.38)	0.54 (0.31)
B42	-10.25	18.83	0.41 (0.47)	0.44 (0.50)	0.44 (1.01)	0.44 (0.95)
D45	-6.56	18.56	0.53 (0.62)	0.55 (0.66)	0.63 (0.88)	2.86 (0.79)
D50	17.75	37.62	0.98 (1.33)	1.12 (1.44)	1.18 (2.34)	1.49 (2.17)

* RMSE and $|y_{max}-y_{min}|$ are for the last 15 days.

** Standard deviations shown in the parentheses are the average for the last 2 days.

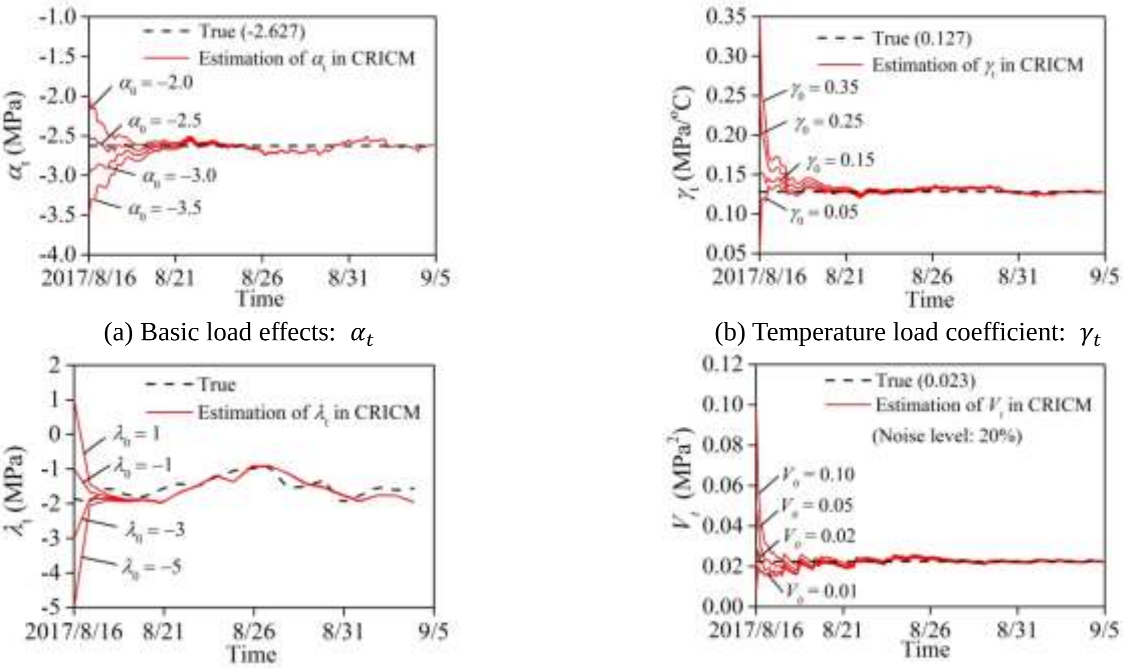

(a) Basic load effects: α_t

(b) Temperature load coefficient: γ_t

(c) Audience load effect: λ_t

(d) Variance of observation noise: V_t

Fig. 8 Effect of different initial guesses for variables in CRICM

4.3.2 Standard deviation and confidence interval

Standard deviations of the predicted responses give an estimation for the uncertainties in the predictions, which are essential to the outlier analysis for damage detection (Zhang *et al.* 2018) and the online structural reliability assessment (Strauss et al. 2008). Table 2 also shows the standard deviations of the predicted stresses (in the parentheses), which are obtained from the variances of the predicted observation ($\sigma_t = \sqrt{Q_t}$) for the last 2 days. The standard deviations are found to be less than 7% in comparison with the ranges of the observations in CRICM and CRIM where the improvement of inference is considered. Fig. 7 also shows the 95% confidence intervals, which indicates that after updating with a few days' data, almost all the measurement data are found to be within the confidence regions by 3 BDLMs except RM. The confidence intervals of CRICM and CRIM are smaller than those of CRM and RM.

4.3.3 Effect of initial value and observational noise

In the present BDLM, the state variables (α_t, γ_t and λ_t) and the variance of the observation noise (V_t) are treated as random variables and updated sequentially using observation data. A parametric study has been conducted to investigate the effect of the initial values for those variables. The results in Fig. 8 show that the state and noise variables converge very well to the true values with wide ranges of initial values, which means that initial values do not affect much on the analysis results.

Fig. 9 shows the RMSE of the predicted stresses for the last 15 days' data and its averaged standard deviation for the last 2 days for various observational noise levels. The RMSE and standard deviation gradually increase as the noise level increases. The results of two methods (CRICM and CRIM), which treat the variance of the observational noise as a random variable, are found to be reasonable and equivalent to the RMSE level. On the other hand, the results

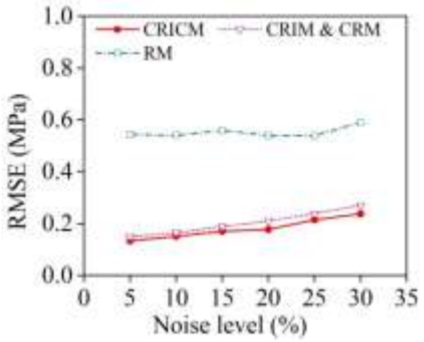

(a) RMSE

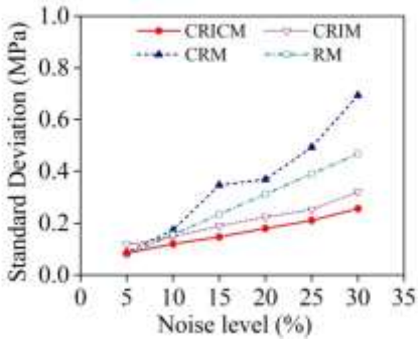

(b) Predicted standard deviation

Fig. 9 RMSE of mean and standard deviation from the probability distribution for C25 with different noise levels

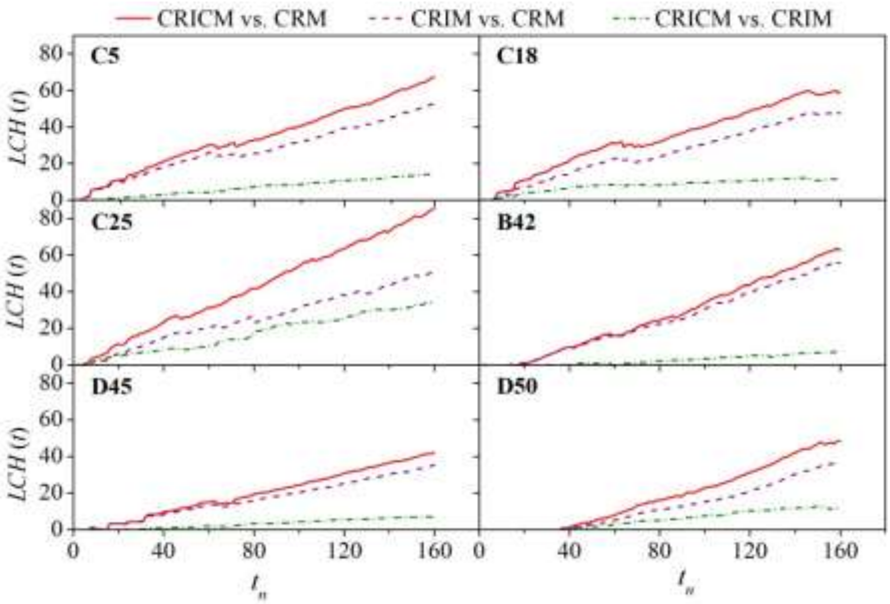

Fig. 10 Log-cumulative Bayes factors LCH(t)

of other two methods (CRM and RM) are not acceptable. The overall performance of CRICM is found to be the best.

4.3.4 Bayes factors

The log-cumulative Bayes factor, LCH, is used to evaluate the performance of the prediction models more comprehensively. Fig. 10 shows three cases of LCH among three models (CRICM vs. CRM, CRIM vs. CRM, and CRICM vs. CRIM) for 6 members. The LCHs are found to be incremental for all cases, which means that the performance of CRICM is the best. The large positive value of LCH of CRIM versus CRM indicates the large contribution of the improved inference for the observation noise variance to the probability distribution of the prediction. For D50 the performance of 3 models is found to be similar for the first 35 data. This is because the stress data on D50 have more variations, making the time to converge longer in the BDLMs.

4.4 Load effect separation

The revolving structure is mainly subjected to three loads, which are the basic, temperature, and audience loads. The stress response caused by these three loads can be separated using Eqs. (6) and (7). The results of the load effect separation for C25 are shown in Fig. 11. They are the posterior (mean) values and standard deviations for the separated load effects.

Figs. 11(a) and 11(b) shows the results for the basic load effect. The mean values by CRICM are found to be consistently close to the true value, while the other results are very erroneous. CRIM and CRM give mean values that wildly fluctuate around the true value because a single overall discount factor is used for the state parameters. RM yields completely incorrect results because the audience influence is not considered separately from the basic load. CRICM gives the smallest standard deviation, indicating the highest confidence in the load effect separation. The temperature load effect can be examined more clearly based

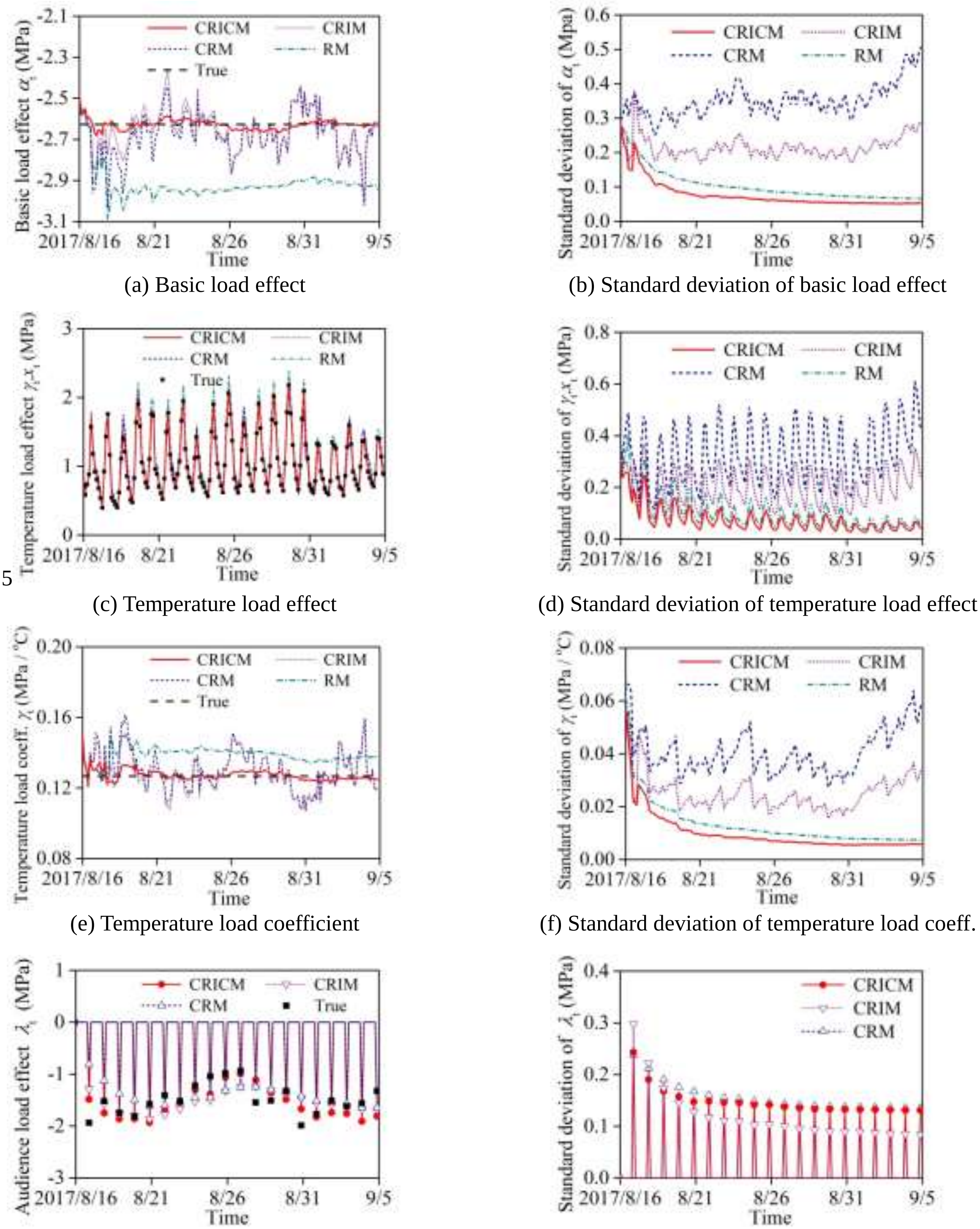

(a) Basic load effect

(b) Standard deviation of basic load effect

(c) Temperature load effect

(d) Standard deviation of temperature load effect

(e) Temperature load coefficient

(f) Standard deviation of temperature load coeff.

(g) Audience load effect

(h) Standard deviation of audience load effect

Fig. 11 Load effect separation results for C25 (based on simulation data)

on the results of the temperature load coefficient γ_t shown in Figs. 11(e) and 11(f) Similar to the basic load effect, the mean values by CRICM are found to be closest to the true value and its standard deviation is smallest. Figs. 11(g)-11(h) shows the results of the audience load effect, which converge reasonably well to the true value after updating for a few days' data by three methods except RM.

Table 3 shows the load effect separation results for the RMSEs and predicted standard deviations on four members by different BDLMs. The results of CRICM are the smallest. CRICM gives much smaller RMSEs in the load effect separation than those of CRIM, although both models give very similar results in the total response predictions. Fig. 12 shows the LCHs of the load effect separation for C25 and

Table 3 Results of the load effect separation: RMSEs and standard deviations (unit: MPa)

Members ($\lvert y_{max}-y_{min}\rvert$*)	BDLMs	Basic Load	Temperature Load	Audience Load
C18 (3.76)	CRICM	0.03** (0.05***)	0.03 (0.06)	0.17 (0.06)
	CRIM	0.13 (0.27)	0.12 (0.23)	0.19 (0.08)
	CRM	0.13 (0.48)	0.12 (0.41)	0.17 (0.14)
	RM	0.30 (0.06)	0.09 (0.05)	—
C25 (3.40)	CRICM	0.02 (0.05)	0.02 (0.04)	0.20 (0.13)
	CRIM	0.12 (0.29)	0.10 (0.24)	0.21 (0.09)
	CRM	0.12 (0.49)	0.10 (0.42)	0.21 (0.14)
	RM	0.29 (0.06)	0.12 (0.05)	—
D45 (18.56)	CRICM	0.06 (0.10)	0.08 (0.13)	0.92 (0.25)
	CRIM	0.25 (0.65)	0.25 (0.55)	0.95 (0.25)
	CRM	0.21 (0.95)	0.24 (0.81)	0.94 (0.27)
	RM	0.87 (0.15)	0.04 (0.12)	—
D50 (37.62)	CRICM	0.16 (0.20)	0.13 (0.18)	0.72 (0.80)
	CRIM	0.90 (2.00)	0.92 (1.68)	0.84 (0.57)
	CRM	0.94 (3.55)	0.92 (3.00)	0.85 (0.82)
	RM	1.17 (2.92)	0.88 (2.48)	—

*$\lvert y_{max}-y_{min}\rvert$ are ranges of the measured total stresses for the last 15 days.
**RMSEs are for the last 15 days.
*** Standard deviations shown in parentheses are averages for the last 2 days.

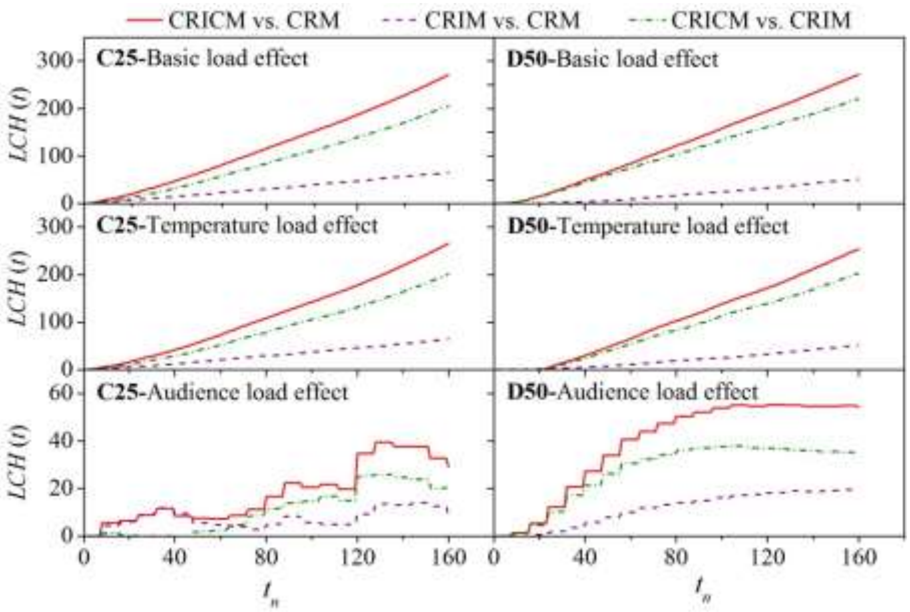

Fig. 12 Log-cumulative Bayes factors for load effect separation: C25 and D50

D50. The LCHs of CRICM versus CRIM show large positive values, which indicates the large benefit of the component discount factors to improve the accuracy of the load effect separation.

5. Analysis of real monitoring data

The performance of the four BDLMs is analyzed for stress response prediction and load separation based on real monitored data on the revolving auditorium for 2 adjacent periods (Period I in 16 August - 5 September 2017 and Period II in 6 September- 26 September 2017). The stress response

Table 4 RMSEs and standard deviations of the predicted stresses (unit: MPa)

Period (2017)	Members	Measured Data		RMSEs of Predictions			
		Mean	$\lvert y_{max}-y_{min}\rvert$	CRICM	CRIM	CRM	RM
Period I (16/8-5/9)	C5	-8.04	13.64	0.65* (1.06**)	0.74 (1.37)	0.76 (3.01)	1.90 (1.99)
	C18	-6.19	9.57	0.65 (1.45)	0.75 (1.60)	0.82 (2.69)	2.19 (1.83)
	C25	-5.62	7.27	0.87 (1.04)	0.91 (1.16)	0.90 (2.63)	1.11 (2.28)
	B42	-2.70	8.43	0.71 (0.94)	0.75 (0.92)	0.78 (1.66)	1.11 (1.56)
	D45	-15.5	8.97	0.59 (0.71)	0.70 (0.84)	0.71 (1.56)	1.20 (1.49)
	D50	-4.02	11.53	0.76 (1.35)	0.86 (1.36)	0.88 (2.63)	1.77 (2.28)
Period II (6/9-26/9)	C5	-8.44	11.64	0.49 (0.52)	0.67 (0.64)	0.68 (1.63)	1.76 (1.42)
	C18	-6.91	8.30	0.55 (0.50)	0.66 (0.63)	0.68 (2.26)	1.62 (1.88)
	C25	-5.25	5.94	0.77 (0.73)	0.84 (0.74)	0.84 (1.42)	1.10 (1.26)
	B42	-2.65	7.68	0.66 (0.61)	0.72 (0.60)	0.77 (1.70)	0.99 (1.45)
	D45	-15.9	9.44	0.54 (0.53)	0.58 (0.60)	0.77 (1.43)	1.29 (1.26)
	D50	-3.56	11.98	0.35 (0.28)	0.34 (0.32)	0.35 (0.52)	1.87 (0.45)

* RMSE and $\lvert y_{max}-y_{min}\rvert$ are for the last 15 days

** Standard deviations shown in the parentheses are the averages for the last 2 days.

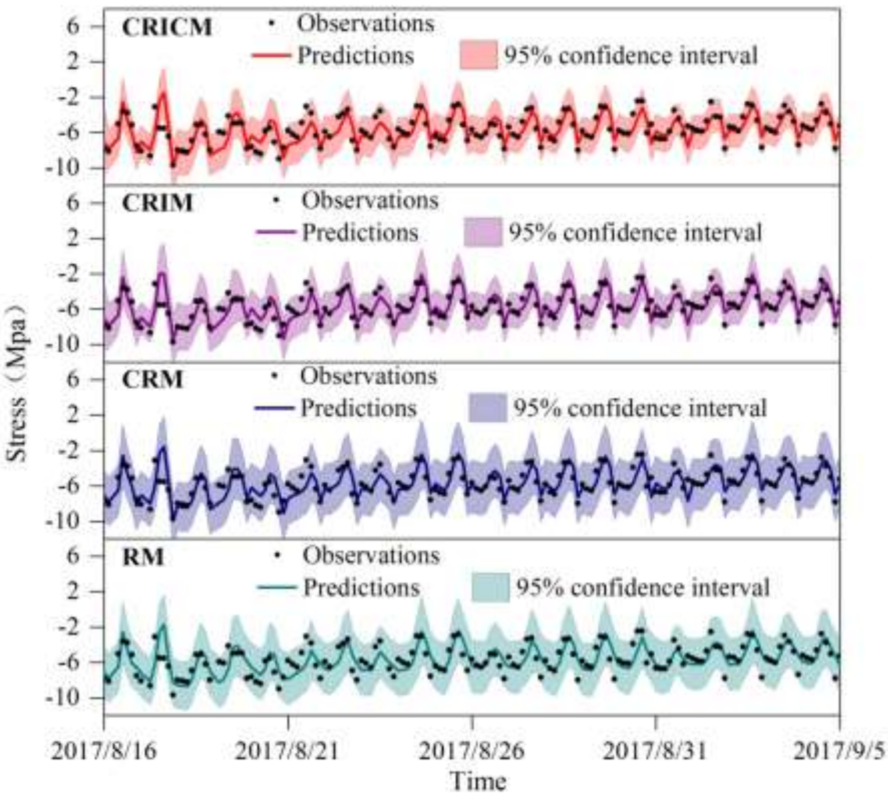

Fig. 13 Response predictions for C25 by four BDLMs based on real monitored data

measurements do not include the self-weight and static load applied to the structure because the sensors were installed after the revolving auditorium was constructed. However, there is still a significant basic load effect because there were some changes after the sensor installation, such as equipment movements and wheel maintenance.

5.1 Prediction of stress response

The initial values for the state variables and the variance of the observational noise are estimated from the first 8 data points: for instance, $m_0' = \langle -8, 0.3, -1.39 \rangle$, $\mathrm{E}(V_0) = 1.0$, and $V_0 \sim \mathrm{IG}(1.5, 0.5)$ for column C25. The first two

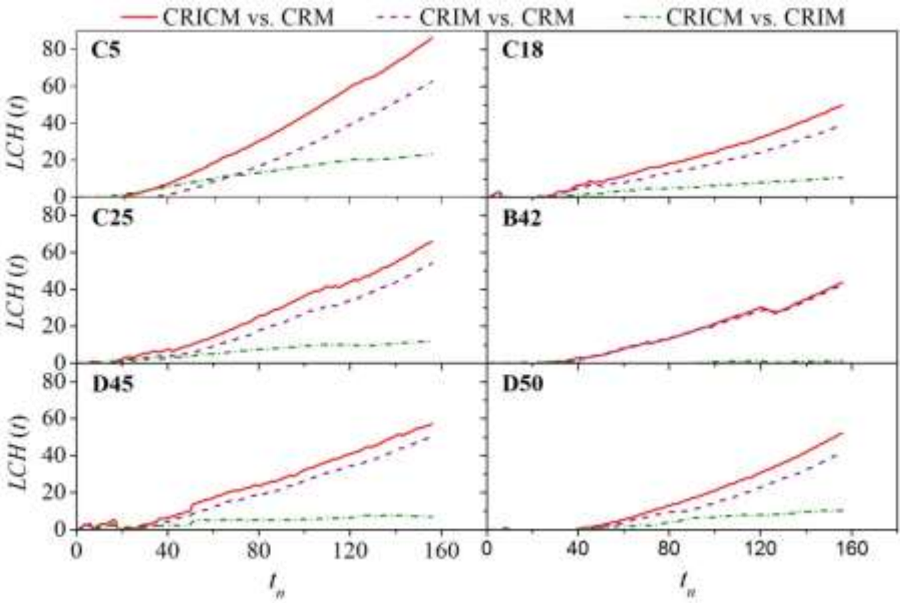

Fig. 14 Log-cumulative Bayes factors LCH(t) for real monitoring data

component discount factors for CRICM are found to be same for six members as $\delta_1 = 0.9$, $\delta_2 = 0.95$. However, the δ_3 values are 0.6, 0.6, 0.75, 0.85, 0.5 and 0.6 for C5, C18, C25, B42, D45, and D50, respectively. The overall discount factors δ for CRIM and CRM are obtained as 0.75, 0.75, 0.8, 0.9, 0.7, and 0.75 for C5, C18, C25, B42, D45, and D50, respectively, whereas those for RM are the same for all members as 0.95.

Fig. 13 shows the predicted results of the stress for C25 by different BDLMs during Period I. The predicted values by CRICM, CRIM and CRM are found to be in good agreement with the measurement data, while those by RM are quite different especially for the cases with audience loads at the end of each day. The 95% confidence intervals show that CRICM gives the smallest intervals.

Table 4 lists the RMSEs of the predicted stresses and the predicted standard deviations for six members by 4 BDLMs during two periods of the measurement. The RMSE and standard deviation levels of the predictions in two different periods are found to be fairly similar, since two periods are adjacent so that the operational and environmental conditions are similar. The RMSEs by CRICM are still smallest, while those by RM are largest. It can also be found that the standard deviations by CRICM are smallest. The RMSE levels and standard deviations of the prediction by CRICM are less than 13% and 16% of the range of the measured data, respectively. The fluctuating amplitudes of the predicted responses and the prediction errors are found to be generally larger in the real monitoring data analyses than those in the simulation study. This may be caused by three factors: additional loads such as wind load, movements of a large number of performers, and revolution angle of the auditorium; larger observation noise; and limitation in the present FE model for accurate stress evaluations.

Fig. 14 shows log-cumulative Bayes factor (LCH) curves for three cases (CRICM vs. CRM, CRIM vs. CRM, and CRICM vs. CRIM) in Period I. Similar to the simulation study, all three LCHs are found to be incremental, which means that the predicted probability distributions by CRICM are better than those by the other two methods. The large positive values for LCH of CRIM versus CRM indicate the big beneficial effects of the improved inference for the observational noise to the probability distribution of the predicted response.

5.2 Load effect separation

Fig. 15 shows the posterior mean values and standard deviations of the load effect separation for C25 in Period I. Figs. 15(a) and 15(b) shows the results of the basic load effect, which shows large fluctuations than the simulated case owing to the higher uncertainty in the operational condition of the revolving auditorium. The results by CRICM are found to be more stable than those by the other two models, and its standard deviation is also smallest. Figs. 15(c) and 15(d) shows the results for the temperature load effect results, which clearly shows a periodical pattern. The results for the temperature load coefficient shown in Figs. 15(e) and 15(f) indicate that CRICM yields the most stable estimates with the smallest standard deviation. Figs. 15(g) and 15(h) shows that the results for the audience load effect by the three models are very similar.

Fig. 16 shows the posterior mean values of the load effect separation for C25 during Period II. The results of the basic and temperature load coefficient are more stable than those for Period I. However, the mean values of the load effect separation are found to be fairly similar to those for Period I, which indicates the consistent performance of the BDLMs, particularly CRICM, on the real monitoring data under similar environmental and operational conditions.

6. Conclusions

In this study, a Bayesian dynamic linear model (BDLM) is presented for data-driven analyses of structure response prediction and load effect separation on a revolving

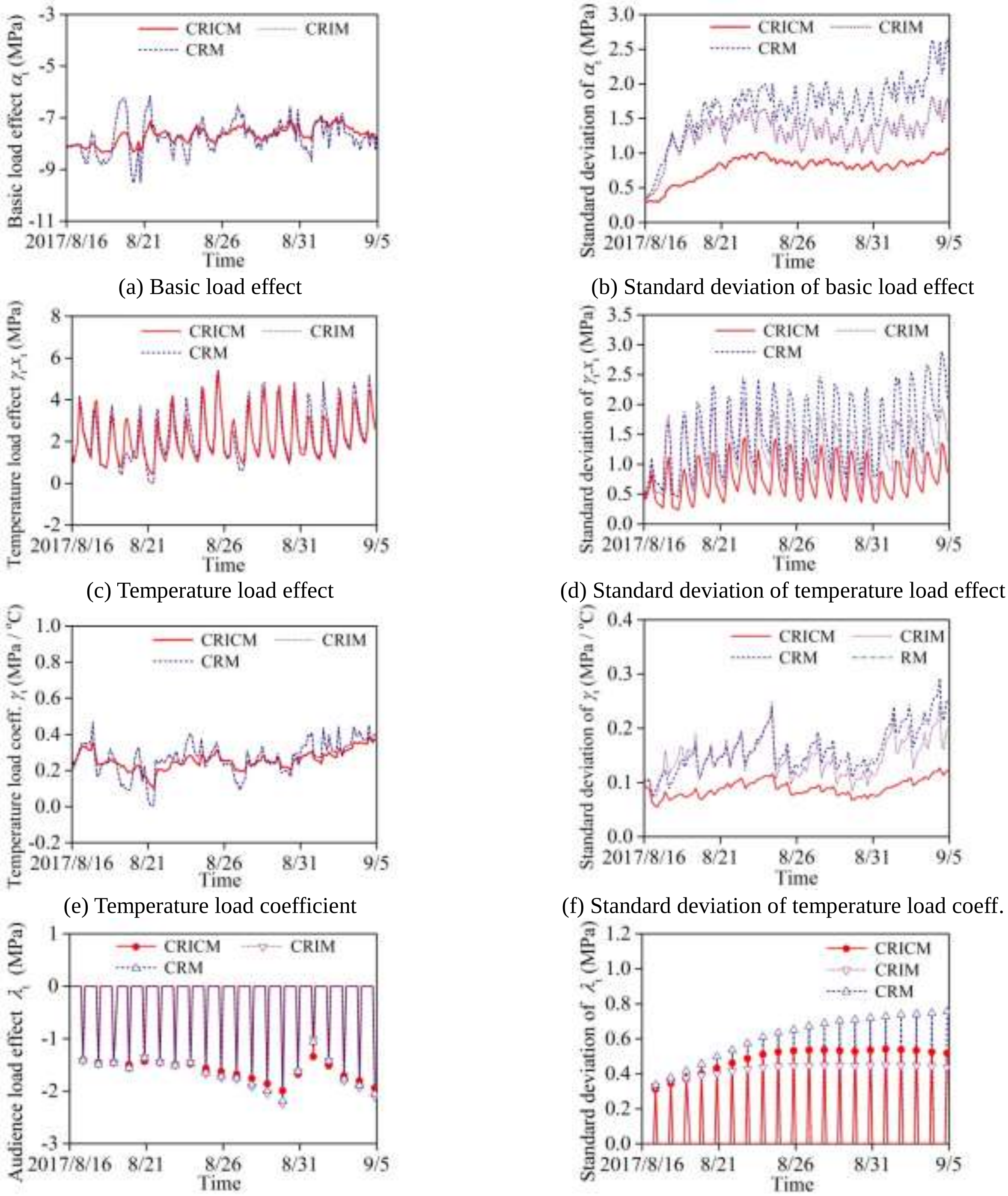

(a) Basic load effect
(b) Standard deviation of basic load effect
(c) Temperature load effect
(d) Standard deviation of temperature load effect
(e) Temperature load coefficient
(f) Standard deviation of temperature load coeff.
(g) Audience load effect
(h) Standard deviation of audience load effect

Fig. 15 Load effect separation results for C25 using real monitored data in Period Ⅰ

auditorium. Three improvements are introduced, which are a classificatory regression component to address the temporary audience load effect, improved inference for the variance of observation noise to be updated continuously, and component discount factors for effective load effect separation. The proposed method is called as the Bayesian classificatory regression model with inference improvement on the observation noise and component discount factors (CRICM).

The performance of the CRICM has been verified based on the simulated data and the real monitoring data on the revolving structure. The results of this study are summarized as follows:

- The classificatory regression component brings significant improvements not only in the load effect separation for the temporary audience but also in the total stress response prediction. The results of the simulation study show that the RMSE levels of the prediction become

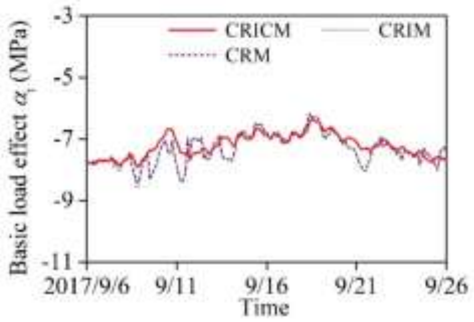

(a) Basic load effect

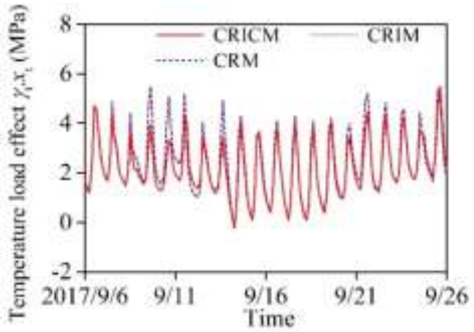

(b) Temperature load effect

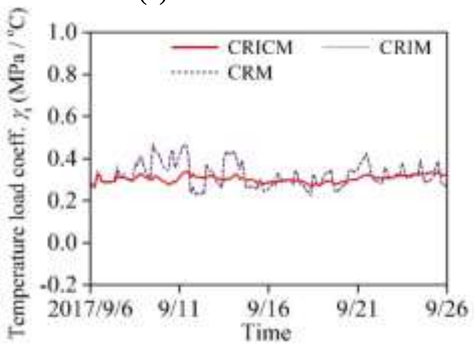

(c) Temperature load effect

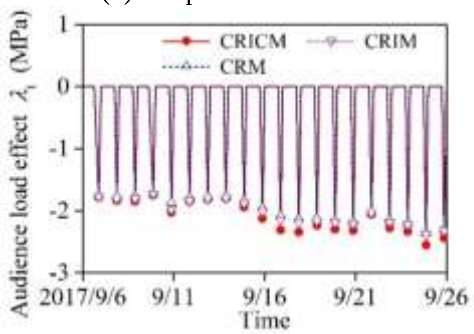

(d) Audience load effect

Fig. 16 Load effect separation results for C25 using real monitored data in Period II

less than 6% of the range of the observations by including the classificatory term.

- The results of Bayes factors indicate that the improved inference for the variance of the observation noise results in a large improvement in the probability distribution of the prediction, which is essential for the outlier identification and reliability assessment of structures. The variance is found to converge to the true value from a wide range of the initially assumed values. The standard deviations of the prediction become less than 7% of the range of the observations by including the improved inference.
- The results of Bayes factors on the separated load effects show that the component discount factors result in significant improvements in the accuracy of the load effect separation.
- The proposed CRICM gives reasonable results for the cases with real monitoring data, although the estimated results show larger errors than the simulation cases owing to the higher uncertainty in the real structural and operation conditions of the revolving auditorium. The RMSE levels and standard deviations for the stress response prediction by CRICM are less than 13% and 16% of the range of the observations, respectively. The results of the total stresses prediction and load effect separation are found to be fairly consistent for the observation data in 2 adjacent periods with similar operational and environmental conditions.

Acknowledgments

The research described in this paper was financially supported by National Key Research and Development Program of China (Grant No. 2017YFC0806100) and National Natural Science Foundation of China (Grant No. 51578491, 51578494 and 51778568).

References

Beck, J.L. (2010), “Bayesian system identification based on probability logic”, *Struct. Control Health Monit.*, **17**(7), 825-847. https://doi.org/10.1002/stc.424.

Brownjohn, J.M.W., Moyo, P., Omenzetter, P. and Lu, Y. (2003), “Assessment of highway bridge upgrading by dynamic testing and finite-element model updating”, *J. Bridge Eng.*, **8**(3), 162-172. https://doi.org/10.1061/(ASCE)1084-0702(2003)8:3(162).

Carden, E.P. and Brownjohn, J.M. (2008), “ARMA modelled time-series classification for structural health monitoring of civil infrastructure”, *Mech. Syst. Signal Pr.*, **22**(2), 295-314. https://doi.org/10.1016/j.ymssp.2007.07.003.

Catbas, F.N., Susoy, M. and Frangopol, D.M. (2008), “Structural health monitoring and reliability estimation: Long span truss bridge application with environmental monitoring data”, *Eng. Struct.*, **30**(9), 2347-2359. https://doi.org/10.1016/j.engstruct.2008.01.013.

Chen, G., Mu, H., Pommerenke, D. and Drewniak, J.L. (2004), “Damage detection of reinforced concrete beams with novel distributed crack/strain sensors”, *Struct. Health Monit.*, **3**(3): 225-243. https://doi.org/10.1177/1475921704045625.

Cho, S., Jo, H., Jang, S., Park, J., Jung, H.J., Yun, C.B., Spencer, B.F. and Seo, J.W. (2010), “Structural health monitoring of a cable-stayed bridge using wireless smart sensor technology: data analyses”, *Smart Struct. Syst.*, **6**(5-6), 461-480. http://dx.doi.org/10.12989/sss.2010.6.5_6.461.

Chung, T.T., Cho, S., Yun, C.B. and Sohn, H. (2012), “Finite element model updating of Canton Tower using regularization technique", *Smart Struct. Syst.*, **10**(4-5), 459-470. http://dx.doi.org/10.12989/sss.2012.10.4_5.459.

Goulet, J.A. (2017), "Bayesian dynamic linear models for structural health monitoring", *Struct. Control Health Monit.*, **24**(12), e2035. https://doi.org/10.1002/stc.2035.

Goulet, J.A. and Koo, K. (2018), "Empirical validation of Bayesian dynamic linear models in the context of structural health monitoring", *J. Bridge Eng.*, **23**(2), 05017017. https://doi.org/10.1061/(ASCE)BE.1943-5592.0001190.

Gul, M. and Catbas, F.N. (2009), "Statistical pattern recognition for Structural Health Monitoring using time series modeling: Theory and experimental verifications", *Mech. Syst. Signal Pr.*, **23**(7), 2192-2204. https://doi.org/10.1016/j.ymssp.2009.02.013.

Hua, X.G., Ni, Y.Q., Chen, Z.Q. and Ko, J.M. (2009), "Structural damage detection of cable-stayed bridges using changes in cable forces and model updating", *J. Struct. Eng.*, **135** (9), 1093-1106. https://doi.org/10.1061/(ASCE)0733-9445(2009)135:9(1093).

Jeffreys, H. (1961), *Theory of Probability*, Oxford University Press, New York, USA.

Jin, C., Li, J., Jang, S., Sun, X. and Christenson, R. (2015), "Structural damage detection for in-service highway bridge under operational and environmental variability", *Sensors and Smart Structures Technologies for Civil, Mechanical, and Aerospace Systems*, **9435**, 94353A. https://doi.org/10.1117/12.2084384.

Jin, S.S. (2019), "Bayesian inference using generalized likelihood for non-traditional residuals", *Eng. Struct.*, **188**, 613-626. https://doi.org/10.1016/j.engstruct.2019.03.062.

Kim, H., Ahn, E., Shin, M. and Sim, S.H. (2018), "Crack and Noncrack Classification from Concrete Surface Images Using Machine Learning", *Struct. Health Monit.*, 1475921718768747.

Kim, J. and Lynch, J.P. (2012), "Experimental analysis of vehicle–bridge interaction using a wireless monitoring system and a two-stage system identification technique", *Mech. Syst. Signal Pr.*, **28**, 3-19. https://doi.org/10.1016/j.ymssp.2011.12.008.

Kim, R.E., Li, J., Spencer, B.F., Nagayama, T. and Mechitov, K.A. (2016), "Synchronized sensing for wireless monitoring of large structures", *Smart Struct. Syst.*, **18**(5), 885-909. http://dx.doi.org/10.12989/sss.2016.18.5.885.

Kromanis, R. and Kripakaran, P. (2016), "SHM of bridges: characterising thermal response and detecting anomaly events using a temperature-based measurement interpretation approach", *J. Civil Struct. Health Monit.*, **6**(2), 237-254.

Lee, J.J., Lee, J.W., Yi, J.H., Yun, C.B. and Jung, H.Y. (2005), "Neural networks-based damage detection for bridges considering errors in baseline finite element models", *J. Sound Vib.*, **280**(3-5), 555-578. https://doi.org/10.1016/j.jsv.2004.01.003.

Lin, Y.Z., Nie, Z.H. and Ma, H.W. (2017), "Structural damage detection with automatic feature - extraction through deep learning", *Comput. -Aided Civil Infrastruct. Eng.*, **32**(12), 1025-1046. https://doi.org/10.1111/mice.12313.

Lindley, D.V. (1972), *Bayesian Statistics, a Review*, SIAM, Philadephia.

Luo, Y.Z., Yang, P.C., Shen, Y.B., Yu, F., Zhong, Z.N. and Hong, J. (2014), "Development of a dynamic sensing system for civil revolving structures and its field tests in a large revolving auditorium", *Smart Struct. Syst.*, **13**(6), 993-1014. http://dx.doi.org/10.12989/sss.2014.13.6.993.

Min, J., Park, S., Yun, C.B. and Song, B. (2010), "Development of a low-cost multifunctional wireless impedance sensor node", *Smart Struct. Syst.*, **6**(5-6), 689-709. http://dx.doi.org/10.12989/sss.2010.6.5_6.689.

Min, J., Park, S., Yun, C.B., Lee, C.G. and Lee, C. (2012), "Impedance-based structural health monitoring incorporating neural network technique for identification of damage type and severity", *Eng. Struct.*, **39**, 210-220. https://doi.org/10.1016/j.engstruct.2012.01.012.

Ni, Y.Q., Li, B., Lam, K.H., Zhu, D., Wang, Y., Lynch, J.P. and Law, K.H. (2011), "In-construction vibration monitoring of a super-tall structure using a long-range wireless sensing system", *Smart Struct. Syst.*, **7**(2), 83-102. http://dx.doi.org/10.12989/sss.2011.7.2.083.

Noh, H.Y., Nair, K.K., Kiremidjian, A.S. and Loh, C.H. (2009), "Application of time series based damage detection algorithms to the benchmark experiment at the National Center for Research on Earthquake Engineering (NCREE) in Taipei, Taiwan", *Smart Struct. Syst.*, **5**(1), 95-117. http://dx.doi.org/10.12989/sss.2009.5.1.095.

Pakzad, S.N. (2010), "Development and deployment of large scale wireless sensor network on a long-span bridge", *Smart Struct. Syst.*, **6**(5-6), 525-543. http://dx.doi.org/10.12989/sss.2010.6.5_6.525.

Rice, J.A., Mechitov, K., Sim, S.H., Nagayama, T., Jang, S., Kim, R., Spencer, B.F., Agha, G. and Fujino, Y. (2010), "Flexible smart sensor framework for autonomous structural health monitoring", *Smart Struct. Syst.*, **6**(5-6), 423-438 http://dx.doi.org/10.12989/sss.2010.6.5_6.423.

Shen, Y., Yang, P., Zhang, P., Luo, Y., Mei, Y., Cheng, H., Jin, L., Liang, C., Wang, Q. and Zhong, Z. (2013), "Development of a multi-type wireless sensor network for the large-scale structure of the national stadium in china", *Int. J. Distrib. Sens. N.*, **9**(12), 709724. https://doi.org/10.1155/2013/709724.

Shinozuka, M., Chou, P.H., Kim, S., Kim, H.R, Karmakar, D. and Lu, F. (2010), "Non-invasive acceleration-based methodology for damage detection and assessment of water distribution system", *Smart Struct. Syst.*, **6**(6), 545-559. http://dx.doi.org/10.12989/sss.2010.6.5_6.545

Siringoringo, D.M. and Fujino, Y. (2009), "Noncontact operational modal analysis of structural members by laser Doppler vibrometer", *Comput.-Aided Civil Infrastruct. Eng.*, **24**(4), 249-265. https://doi.org/10.1111/j.1467-8667.2008.00585.x.

Skolnik, D., Lei, Y., Yu, E. and Wallace, J.W. (2006), "Identification, model updating, and response prediction of an instrumented 15-story steel-frame building", *Earthq. Spectra*, **22**(3), 781-802. https://doi.org/10.1193/1.2219487.

Sohn, H. (2006), "Effects of environmental and operational variability on structural health monitoring", *Philosophical Transactions of the Royal Society of London A: Mathematical, Physical and Engineering Sciences*, **365**(1851), 539-560. https://doi.org/10.1098/rsta.2006.1935.

Strauss, A., Frangopol, D.M. and Kim, S. (2008), "Use of monitoring extreme data for the performance prediction of structures: Bayesian updating", *Eng. Struct.*, **30**(12), 3654-3666. https://doi.org/10.1016/j.engstruct.2008.06.009.

Wan, H.P. and Ni, Y.Q. (2018a), "Bayesian modeling approach for forecast of structural stress response using structural health monitoring data", *J. Struct. Eng.*, **144**(9), 04018130. https://doi.org/10.1061/(ASCE)ST.1943-541X.0002085.

Wan, H.P. and Ni, Y.Q. (2018b), "Bayesian multi-task learning methodology for reconstruction of structural health monitoring data", *Struct. Health Monit.*, 1475921718794953.

Wang, H., Zhang, Y.M., Mao, J.X., Wan, H.P., Tao, T.Y. and Zhu, Q.X. (2019), "Modeling and forecasting of temperature-induced strain of a long-span bridge using an improved Bayesian dynamic linear model", *Eng. Struct.*, **192**, 220-232. https://doi.org/10.1016/j.engstruct.2019.05.006.

Wang, J. and Liu, X. (2010), "Evaluation and Bayesian dynamic prediction of deterioration of structural performance", *Struct. Infrastruct. Eng.*, **6**(6), 663-674. https://doi.org/10.1080/15732470701478503.

Wang, Y.C., Luo, Y.Z., Sun, B., Liu, X., Jia, Z.X. and Shen Y.B. (2018), "Field measurement system based on a wireless sensor network for the wind load on spatial structures: Design, experimental, and field validation", *Struct. Control Health Monit.*, **25**(9), e2192. https://doi.org/10.1002/stc.2192.

West, M. and Harrison, J. (1997), *Bayesian Forecasting and Dynamic Models*. Springer, New York, USA.

Wu, J., Tang, Z., Lv, F., Yang, K., Yun, C.B. and Duan, Y. (2018), "Ultrasonic guided wave-based switch rail monitoring using independent component analysis", *Measure. Sci. Technol.*, **29**(11), 115102.

Xia, Y., Chen, B., Weng, S., Ni, Y.Q. and Xu Y.L. (2012), "Temperature effect on vibration properties of civil structures: a literature review and case studies", *J. Civil Struct. Health Monit.*, **2**(1), 29-46.

Xu, Y.L., Chen, B., Ng, C.L., Wong, K.Y. and Chan, W.Y. (2010). "Monitoring temperature effect on a long suspension bridge", *Struct. Control Health Monit.*, **17**(6), 632-653. https://doi.org/10.1002/stc.340.

Yun, C.B. and Bahng, E.Y. (2000), "Substructural identification using neural networks", *Comput. Struct.*, **77**(1), 41-52. https://doi.org/10.1016/S0045-7949(99)00199-6.

Zhang, L.H., Wang, Y.W., Ni, Y.Q. and Lai, S.K. (2018), "Online condition assessment of high-speed trains based on Bayesian forecasting approach and time series analysis", *Smart Struct. Syst.*, **21**(5), 705-713. https://doi.org/10.12989/sss.2018.21.5.705.

Zhang, Z.Y. and Luo, Y.Z. (2017), "Restoring method for missing data of spatial structural stress monitoring based on correlation", *Mech. Syst. Signal Pr.*, **91**, 266-277. https://doi.org/10.1016/j.ymssp.2017.01.018.

Zheng, H. and Mita, A. (2008), "Damage indicator defined as the distance between ARMA models for structural health monitoring", *Struct. Control Health Monit.*, **15**(7), 992-1005. https://doi.org/10.1002/stc.235.

Zhu, B. and Frangopol, D.M. (2013), "Incorporation of structural health monitoring data on load effects in the reliability and redundancy assessment of ship cross-sections using Bayesian updating", *Struct. Health Monit.*, **12**(4), 377-392. https://doi.org/10.1177/1475921713495082.

Zhu, Y., Ni, Y.Q., Jesus, A., Liu, J. and Laory, I. (2018), "Thermal strain extraction methodologies for bridge structural condition assessment", *Smart Mater. Struct.*, **27**(10), 105051.

Zhu, Y., Ni, Y.Q., Jin, H., Inaudi, D. and Laory, I. (2019), "A temperature-driven MPCA method for structural anomaly detection", *Eng. Struct.*, **190**, 447-458. https://doi.org/10.1016/j.engstruct.2019.04.004.

Zonta, D., Wu, H., Pozzi, M., Zanon, P., Ceriotti, M., Mottola, L., Picco, G.P., Murphy, A.L., Guna, S. and Corrá, M. (2010), "Wireless sensor networks for permanent health monitoring of historic buildings", *Smart Struct. Syst.*, **6**(5-6), 595-618. http://dx.doi.org/10.12989/sss.2010.6.5_6.595.

HJ